18th International Conference on Information Fusion
Washington, DC - July 6-9, 2015

New Algorithms for Daylight Harvesting in a Private Office

Rohit Kumar
Lighting Solutions and Services
Philips Research North America
Briarcliff Manor, NY 10510
Rohit.Kumar@Philips.com

Abstract – *A daylight harvesting system can produce almost* 60% *energy saving by using daylight to satisfy illumination requirements. In this paper we study the problem of daylight harvesting for an indoor office which has adjustable electric lights and blinds. There are two main problems with such a system namely; a) photo sensor should ideally be placed on the work desk to measure illumination. However such a sensor can be accidently covered by paper or occluded by user leading inaccurate measurements b) changing daylight distribution inside the room due to movement of sun and window blinds. New data fusion algorithms are proposed in this paper that employ machine learning and radiosity theory to compute the electric light and daylight component (hence total illuminance) on the work plane using ceiling mounted sensor. Experimental results from a real test bed are provided at the end to highlight the performance of each algorithm.*

Keywords: Daylight Harvesting, Intelligent Lighting Systems, Energy Savings.

1 Introduction

The problem of daylight harvesting is well-known and well-researched in lighting community [1, 2, 3, 4]. The goal of the problem is to maximize the use of daylight to satisfy illumination demands and thereby minimize the use of electricity. In this paper we study the daylight harvesting problem for an office environment as shown in Fig. 1(a) where the goal is to maintain constant illumination on the work desk (a.k.a. work plane). A general daylight harvesting system consists of photo sensor which measures the illumination, and a controller which uses the measurements from photo sensor to adjust the electric light. One can basically have two types of controllers in this set up: a) Open-loop controller: In case of an open-loop controller, the system adjusts the luminance inside the room based on some external parameters or sensors. Generally, a sensor is placed outside the room (such as on the window) which measures the daylight falling on the window. The controller adjusts the artificial (electric) light based on luminance on the window and it does not have any information about the illuminance inside the room, and b) Closed-loop controller: In case of closed-loop controller, a sensor is placed inside the room. As expected, the presence of the sensor inside the room provide illuminance inside the room and is more accurate to control the artificial light [5, 6].

Ideally, in case of a closed-loop controller, the sensor should be placed on the work desk to measure the true illumination. This information can then be fed to the controller to adjust the artificial light to meet the illuminance demand. However a sensor on the work desk can be accidently covered by files, paper, or user himself leading to inaccurate measurement [8]. These measurements are fed to the controller which adjust the artificial light incorrectly resulting in a failed system. Hence, as largely accepted by the lighting community, sensor should be mounted on the ceiling or on the wall. With the sensor mounted on the roof and not on the area of interest (work desk), it requires advanced algorithms to estimate the illumination on the work plane based on these ceiling/wall mounted sensors.

Fig. 1(b) shows a office set up with ceiling mounted sensor. The sensor measures the illumination due to daylight and artificial light in the room. While artificial light is relatively static and can be computed accurately, daylight is more dynamic and varies a lot. The amount of light falling on the work plane is not only dependent on the outside light but also on the status of blinds, i.e., blind height and blind angle. For instance, even if there is lot of daylight falling on the window and blinds are positioned to block sunlight, the amount of daylight in the room will be minimal and vice-versa. In initial work, researchers tried to develop an illumination ratio to correlate external daylight to the illumination on the work plane [2, 3]. However, one correlation ratio was unable to model changing dynamics of the sunlight in the room. Therefore, other researchers in [7] developed multiple illumination ratios for different blind angles (30, 40, 50 and 60 degrees). The discrete limits imposed by these authors prevents the system from exploiting overall range of blinds. This drawback was addressed in [8] wherein authors have developed a clustering technique to model the daylight inside the room more accurately. Consequently, the number of ratios developed in this case is not determined a priori but is dependent on the location of the window and status of the blinds. We shall employ their clustering technique and develop new data fusion algorithms to better estimate the illuminance falling on the work plane.

The paper is organized as follows: Section 2 details the experimental set and the problem statement for this research. Section 3 develops relation between the illumination between work plane and measurements by the sensors. These relations are employed to develop several data fusion algorithms in Section 4. Section 5 has experimental results to highlight the performance of different algorithms and the paper ends with conclusion and directions for future work in Section 6.

2 Problem Set Up

In this section, we shall describe the experimental set up for our daylight harvesting system and then formulate the estimation problem.

2.1 Experiment Set Up

The experimental set up for a private office is shown in Figure 2. The set up consists of the following components:

1. Sensors: We shall employ three sensors in this system to measure illumination. Two sensors (C_0 and C_1) are mounted on ceiling inside the room while one sensor (C_2) is placed on the window facing outward (towards the sky). Note that ceiling sensors are not necessarily located directly over the work plane. It only measures the illumination in the room while window sensor only measures daylight falling on the window and cannot measure illumination in the room.

2. Light Fixtures: There are two light fixtures (L_0, L_1) with adjustable ballast. Ballast level for each light fixture can be varied between 0 to 255.

3. Blinds: Room has one large window that is fitted with moveable blinds. Height (b_h) and tilt (angle)(b_θ) of the blinds can be adjusted to maximize the amount of light falling in the room without causing glare to the user. Therefore, the light falling on the window as measured by window sensor may not be equal to daylight illumination on the work plane.

4. Controller: In our current set up, we have one open-loop and one closed-loop controller running. The open-loop controller adjusts the blind height (b_h) and blind angle (b_θ) based on direction of the window and movement of sun. The open-loop controller adjusts the blinds to maximize the daylight in the room without causing discomfort (glare) to the user [9, 8]. The closed-loop controller adjusts the ballast level for light fixtures (L_0, L_1) to satisfy the illumination requirements. Since controller is not the focus of this paper, we shall not delve into details of controller. We shall consider it as a black box which outputs the adjustable ballast levels given the sensor measurements.

Notation: In order to eliminate excessive notations, we shall abuse the notation slightly. We shall use C_i to indicate i^{th} sensor ($i \in \{0,1\}$). It will also be used to indicate its measurements. The reference will be clear from the context. We shall use a similar strategy for artificial lighting ($L_j, j \in \{0,1\}$). $C_i(L_1, L_2)$ indicates measurement of i^{th} ceiling sensor in presence of artificial lights which are set at level L_1 and L_2. $C_i(L_j)$ indicates measurement of i^{th} ceiling sensor in presence of j^{th} light fixture which is set at level L_j. The other light is assumed to be turned off. $C_i(C_2, b_h, b_\theta)$ indicates measurements of i^{th} ceiling sensor in presence of daylight where daylight falling on window is C_2, and blind status is (b_h, b_θ). $C_i(C_2, b_h, b_\theta, L_1, L_2)$ indicates measurements of i^{th} ceiling sensor in presence of artificial light and daylight. We wish to emphasize that $C_i(x)$ is not a function. It only indicates ceiling sensor measurements in presence of x (x can be daylight parameters (C_2, b_h, b_θ) or ballast levels for artificial lights (L_1, L_2)).

2.2 Problem Formulation

The total illuminance (I_W) on work plane is given as:

$$I_W = f(L_0, L_1, C_2, b_h, b_\theta) \tag{1}$$

where f is some unknown function. However from theory of radiosity [8], we know that total illumination on the plane is linear combination of light emitted from different light sources. Therefore,

$$\begin{aligned} I_W &= f_e(L_0, L_1) + f_d(C_2, b_h, b_\theta) \\ &= I_E + I_D \end{aligned} \tag{2}$$

where f_e is a function that maps the given ballast levels to illumination (I_E, i.e., electric light component) on work plane, and f_d is a function that maps the outside light and status of blinds to illumination (I_D, i.e., daylight component) on work plane. The overall five dimensional function approximation problem reduces to two function approximation problem of smaller size. The dimension reduction is critical not only for reducing computation load but also provides better understanding of the system for fault detection and diagnosis.

Hence, the goal of this estimation problem is to estimate daylight (f_d) and electric light (f_e) component based on the available sensor measurements.

3 Relationship between work plane illumination and sensor measurements

In this section we shall define relationships (to be employed in next section) to address the challenge of estimating the illuminance on the work plane without placing a sensor on it. In particular, we shall we place an auxiliary sensor (called as hobo sensor and shall be denoted by h) on the

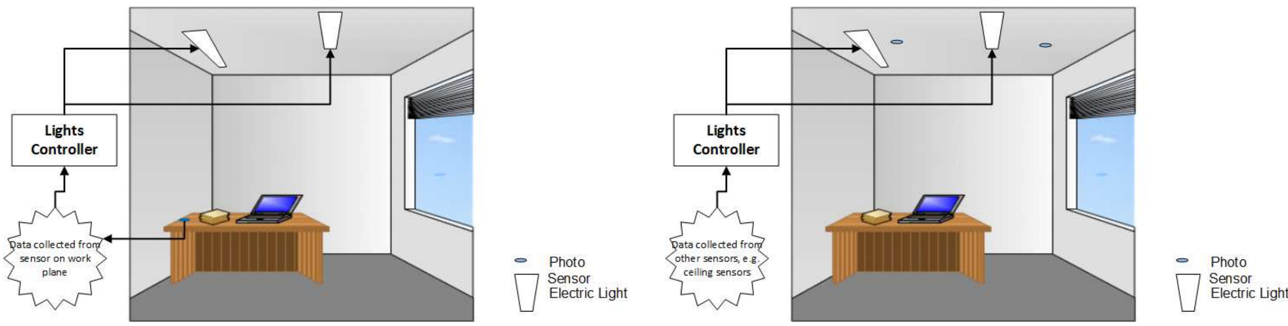

(a) (b)

Figure 1: Workplane illumination estimation set up (a) using a sensor on the desk (b) using ceiling mounted sensors

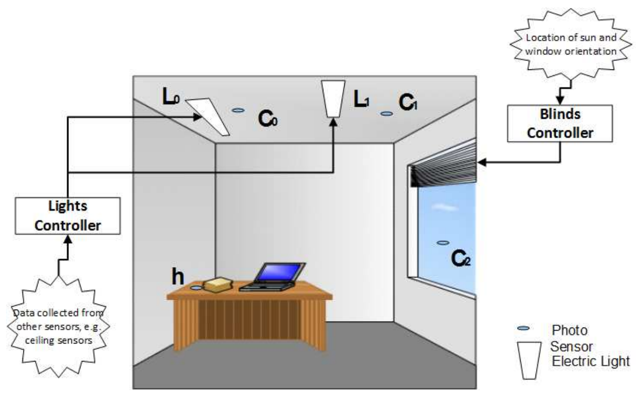

Figure 2: Experiment Set Up.

work plane during data collection phase and then perform supervised learning [10, 11] to estimate the relation between illuminance falling on the work plane (as measured by hobo) and measured by the ceiling sensors. As mentioned earlier, the illuminance falling on the work plane is a combination of daylight and electric light. Therefore, we shall estimate the aforementioned relationships for both.

We wish to highlight that hobo sensor is only used during the learning phase of the set up and is not foreseen to be part of the final product. For hobo sensor, we shall the notation similar to ceiling sensor where $h(x)$ will indicate reading by hobo sensor in presence of x (x can be daylight parameters (C_2, b_h, b_θ) or ballast levels for artificial lights (L_0, L_1)).

3.1 Relationship for artificial light

First, we shall derive relationships for artificial light, i.e., electric lights. In particular, given the status of ballast levels for each light fixtures, we shall develop its relationship to true illumination on the work plane (as measured by hobo sensor) and measurement by ceiling sensors. Before we define the experimental details, we shall outline some relationships that are used in computations later.

Note that total illuminance on the work plane as measured by hobo sensor will be given as:

$$f_e(L_0, L_1) = h(L_0, L_1)$$

Again using radiosity theory, we further reduce two-dimensional function to one-dimensional as follows:

$$h(L_0, L_1) = h(L_0) + h(L_1) \tag{3}$$

i.e., the total illumination on the work plane (as measured by hobo) for given ballast levels of light fixtures is equal additive in nature. Hence, it is equal to sum of illuminance contributed by each luminaries. Further, one can develop similar relationship for ceiling sensors as given below:

$$C_0(L_0, L_1) = C_0(L_0) + C_0(L_1) \tag{4}$$

$$C_1(L_0, L_1) = C_1(L_0) + C_1(L_1) \tag{5}$$

We shall describe the procedure for function approximation $h(L_0)$ and $h(L_1)$, i.e, illuminance on the work plane (as measured by hobo sensor) for given ballast level (L_1, L_2) of the light fixtures. Similar process can be repeated for ceiling sensors as well (i.e., for $C_i(L_j), \forall i, j \in \{0, 1\}$). The function approximation is performed in three steps:

1. Data Collection: Data collection process is performed at night (in absence of daylight). Set $L_1 = 0$ (switch

off). Vary L_0 from 0 to 255 in steps of 5 and collect measurements for hobo sensor for each ballast level. Therefore, we have $\{h_0^m, L_0^m\}_{m=1}^M$, M measurements where L_0^m indicates the ballast level and h_0^m indicates the corresponding illuminance on the work plane as measured by hobo sensor. Then repeat the experiment for L_1 with $L_0 = 0$ and collect $\{h_1^m, L_1^m\}_{m=1}^N$ N data points.

2. Clustering: A manual review of collected data shows that hobo measurements form piecewise linear function of ballast levels. There will be three linear links as shown in Fig 3) and shall be parameterized using following equations:

$$h(L_0) = u_{00}^r L_0 + v_{00}^r \quad (6)$$
$$h(L_1) = u_{01}^r L_1 + v_{01}^r \quad (7)$$

where

$$r = \begin{cases} 1 & \text{if} \quad L_0 \leq n_1; \\ 2 & \text{if} \quad n_1 < L_0 \leq n_2; \\ 3 & \text{if} \quad L_0 > n_2. \end{cases}$$

The parameters $u_{00}^r, v_{00}^r, u_{01}^r, v_{01}^r$ will be estimated using data collected in Step 1. We select $n_1 = 30$ and $n_2 = 210$. Although n_1 and n_2 are selected manually, it can be easily automated. Based on the given thresholds (n_1 and n_2), the cluster the data into three groups as follows:

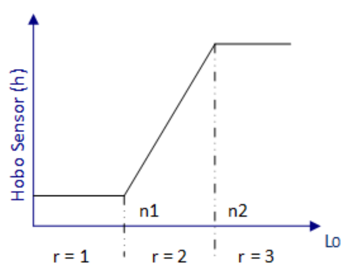

Figure 3: Example for relation between true illumination between on work plane for given ballast level

$$\{h_0^m, L_0^m\}_{m=1}^{M_1} \text{ if } L_0^m < n_1$$
$$\{h_0^m, L_0^m\}_{m=1}^{M_2} \text{ if } n_1 \leq L_0^m \leq n_2$$
$$\{h_0^m, L_0^m\}_{m=1}^{M_3} \text{ if } n_2 \geq L_0^m$$

$$\{h_1^m, L_1^m\}_{m=1}^{N_1} \text{ if } L_1^m < n_1$$
$$\{h_1^m, L_1^m\}_{m=1}^{N_2} \text{ if } n_1 \leq L_1^m \leq n_2$$
$$\{h_1^m, L_1^m\}_{m=1}^{N_3} \text{ if } n_2 \geq L_1^m \qquad .$$

where $M_1 + M_2 + M_3 = M$ and $N_1 + N_2 + N_3 = N$

3. Regression: Perform linear regression to estimate the unknown parameters in Eqn. (6) and (7).

$$(u_{00}^r, v_{00}^r) = \underset{a,b}{\operatorname{argmin}} \sum_{m=1}^{M_r} \{h_0^m - (aL_0^m + b)\}^2$$
$$(u_{01}^r, v_{01}^r) = \underset{a,b}{\operatorname{argmin}} \sum_{m=1}^{N_r} \{h_1^m - (aL_1^m + b)\}^2$$

Therefore, Eqn. (6) and (7) maps the given ballast level of light fixtures to illumination on the work desk.

Additionally, one can also find relation between given ballast level and light measured by ceiling sensors, i.e., one can estimate following relationships:

$$C_0(L_0) = a_{00}^r L_0 + b_{00}^r \quad (8)$$
$$C_0(L_1) = a_{01}^r L_1 + b_{01}^r \quad (9)$$
$$C_1(L_0) = a_{10}^r L_0 + b_{10}^r \quad (10)$$
$$C_1(L_1) = a_{11}^r L_1 + b_{11}^r \quad (11)$$

3.2 Relationship for daylight

Similar to previous subsection, we shall derive the relation between illumination on work plane and ceiling sensor for daylight in the room. The amount of daylight in the room is determined by daylight falling on the window (C_2) and blind status (b_h, b_θ).

1. Data Collection: Large number of measurements were collected for $\{C_0^m, C_1^m, C_2^m \text{ and } h^m\}_{m=1}^M$ for various combinations of (b_h, b_θ). b_h is varied using solar position and b_θ is some control to maximize the amount of sunlight in the room and yet avoiding glare. The electric lights were switched off during data collection. Subsequently we perform clustering and regression analysis.

2. Clustering: Cluster the observed data based on various combinations of (b_h, b_θ, C_2), i.e., $\left\{\{C_0^m, C_1^m, C_2^m, h^m\}_{m=1}^{M_c}\right\}_{c=1}^K$ where there are K clusters such that c^{th} cluster has M_c data points. Interested readers are referred to work of [9] for details about clustering.

3. Regression: We assume that there exists a linear relationship between the following quantities:

$$C_0(C_2, b_h, b_\theta) = \alpha_0^c C_2 + \beta_0^c \quad (12)$$
$$C_1(C_2, b_h, b_\theta) = \alpha_1^c C_2 + \beta_1^c \quad (13)$$
$$h(C_2, b_h, b_\theta) = \alpha_h^c C_2 + \beta_h^c \quad (14)$$
$$h(C_2, b_h, b_\theta) = \alpha_m^c C_0(C_2, b_h, b_\theta) + \beta_m^c C_1(C_2, b_h, b_\theta) \quad (15)$$

where superscript c indicates the cluster index. $C_0(C_2, b_h, b_\theta), C_1(C_2, b_h, b_\theta), h(C_2, b_h, b_\theta)$ represent the daylight measurement by ceiling sensor and hobo sensor respectively. Note that for given cluster, Eqn. (12)-(15) maps the window sensor measurements to ceiling sensors, Eqn. (14) maps it to illumination on work plane. Eqn. (15) maps the ceiling sensor measurements to true illumination on the work plane.

The regression parameters for the above equation can be computed using simple linear least square. For instance, Eqn. (12) parameters can be computed using equation below:

$$(\alpha_0^c, \beta_0^c) = \underset{a,b}{\operatorname{argmin}} \sum_{m=1}^{M_c} \{C_0^m - (aC_2^m + b)\}^2$$

Similar optimization can be performed for Eqns.(13)-(15). Next, we rewrite Eqn. (15) in matrix form

$$h(C_2, b_h, b_\theta) = I_D = \mathbf{k}_2^{c\,T} \mathbf{C}_D \tag{16}$$

where $\mathbf{k}_2^c = \begin{bmatrix} \alpha_m^c \\ \beta_m^c \end{bmatrix}$ and $\mathbf{C}_D = \begin{bmatrix} C_0(C_2, b_h, b_\theta) \\ C_1(C_2, b_h, b_\theta) \end{bmatrix}$

4 Algorithms

Under the normal working conditions, the ceiling sensor measurements will be a combination of contribution due to artificial light and daylight, i.e

$$C_i(C_2, b_h, b_\theta, L_0, L_1) = C_i(C_2, b_h, b_\theta) + C_i(L_0, L_1) \tag{17}$$

where $i \in \{0, 1\}$. Now we shall employ different relationships developed in earlier section to fuse information from different sensor and estimate the illumination on the work plane.

4.1 Algorithm I

In this algorithm, we determine illumination due to electric light (I_E) using relation in Eqn. (6)-(7). The daylight component (I_D) is a two step process: first we compute the daylight component in ceiling sensor measurement using Eqn. (17), then Eqn. (15) is used to compute daylight illumination on work plane. Since artificial light estimation is based on training, there is no feedback mechanism to determine a faulty bulb (in which case there is zero illuminance for any ballast level). This is the main drawback of this algorithm. The steps for Algorithm I are given in Table 1.

4.2 Algorithm II

In Algorithm II, we compute the electric light component using relation in (6), (7) and employ window sensor to compute the daylight component as in (14). The main advantage of this algorithm is that daylight and electric light component are computed independently. Hence the estimation error in one is not propagated. There are two drawbacks on this algorithm, i.e., similar to Algorithm 1, it is unable to determine a faulty bulb in the room and since this algorithms is not using ceiling sensor at all, true illuminance of room is unknown. The steps for Algorithm II are given in Table 2.

1. Given $C_i(C_2, b_h, b_\theta, L_0, L_1), L_i, C_2, b_h, b_\theta, i \in \{0, 1\}$.
2. Compute I_E using (6), (7) and (3).
3. Compute $C_0(L_0, L_1)$ using Eqns.(8), (9), (4), and $C_1(L_0, L_1)$ using Eqns.(10), (11), (5).
4. Compute
$$C_0(C_2, b_h, b_\theta) = C_0(C_2, b_h, b_\theta, L_0, L_1) - C_0(L_0, L_1)$$
$$C_1(C_2, b_h, b_\theta) = C_1(C_2, b_h, b_\theta, L_0, L_1) - C_1(L_0, L_1)$$
5. If $C_i(C_2, b_h, b_\theta) < 0$ then set it equal to zero $\forall i \in \{0, 1\}$.
6. Compute current cluster index c using C_2, b_h, b_θ.
7. Compute I_D using Eqn. (15).
8. $I_W = I_E + I_D$.

Table 1: Steps for Algorithm I

1. Given $L_0, L_1, C_2, b_h, b_\theta$.
2. Compute I_E using Eqns.(6), (7) and (3).
3. Compute current cluster index c using C_2, b_h, b_θ.
4. Compute I_D using Eqn. 14.
5. $I_W = I_E + I_D$.

Table 2: Steps for Algorithm II

4.3 Algorithm III

Before we go into details of this algorithm, we rewrite Equations (6)-(11) using matrix notations:

$$\begin{aligned} \begin{bmatrix} C_0(L_0, L_1) \\ C_0(L_0, L_1) \end{bmatrix} &= \begin{bmatrix} a_{00}^r & a_{01}^r \\ a_{10}^r & a_{11}^r \end{bmatrix} \begin{bmatrix} L_0 \\ L_1 \end{bmatrix} + \begin{bmatrix} b_{00}^r + b_{01}^r \\ b_{10}^r + b_{11}^r \end{bmatrix} \\ h(L_0, L_1) &= \begin{bmatrix} a_0^r & a_1^r \end{bmatrix} \begin{bmatrix} L_0 \\ L_1 \end{bmatrix} + \begin{bmatrix} b_0^r + b_1^r \end{bmatrix} \end{aligned}$$

Define

$$\mathbf{C}_E = \begin{bmatrix} C_0(L_0, L_1) \\ C_0(L_0, L_1) \end{bmatrix}, \mathbf{L} = \begin{bmatrix} L_0 \\ L_1 \end{bmatrix}, \mathbf{V}_s = \begin{bmatrix} a_{00}^r & a_{01}^r \\ a_{10}^r & a_{11}^r \end{bmatrix}$$

$$\mathbf{p} = \begin{bmatrix} b_{00}^r + b_{01}^r \\ b_{10}^r + b_{11}^r \end{bmatrix} \mathbf{a} = \begin{bmatrix} a_0^r & a_1^r \end{bmatrix}^T, \mathbf{b} = \begin{bmatrix} b_0^r + b_1^r \end{bmatrix}$$

Therefore rewriting the earlier equation we get,

$$\begin{aligned} \mathbf{C}_E &= \mathbf{V}_s \mathbf{L} + \mathbf{p} \\ h(L_0, L_1) &= \mathbf{a}^T \mathbf{L} + \mathbf{b} \\ &= \mathbf{a}^T \mathbf{V}_s^{-1} (\mathbf{C}_E - \mathbf{p}) + \mathbf{b} \\ &= \mathbf{k}^T (\mathbf{C}_E - \mathbf{p}) + \mathbf{b} \\ &= \mathbf{k}^T \mathbf{C}_E - \mathbf{k}^T \mathbf{p} + \mathbf{k}^T \mathbf{b} \end{aligned}$$

Therefore, the electric light illuminance on the work plane can be expressed in terms of ceiling sensor values. For the given experiment, we find the $-\mathbf{k}^T \mathbf{p} + \mathbf{k}^T \mathbf{b}$ is very small and hence will be neglected. Therefore,

$$h(L_0, L_1) = I_E = \mathbf{k}^T \mathbf{C}_E \tag{18}$$

In this algorithm, the daylight component is computed using the window sensor. The electric light computation is a three step process: first compute the daylight sensed by the ceiling sensor, next compute the electric component of the ceiling

1. Given $C_i(C_2, b_h, b_\theta, L_0, L_1), L_i, C_2, b_h, b_\theta, i \in \{0,1\}$.
2. Compute current cluster index c using C_2, b_h, b_θ.
3. Compute I_D using (14).
4. Compute $C_0(C_2, b_h, b_\theta)$ using Eqn. (12) and $C_1(C_2, b_h, b_\theta)$ using Eqn. (13).
5. Compute
$$C_0(L_0, L_1) = C_0(C_2, b_h, b_\theta, L_0, L_1) - C_0(C_2, b_h, b_\theta)$$
$$C_1(L_0, L_1) = C_1(C_2, b_h, b_\theta, L_0, L_1) - C_1(C_2, b_h, b_\theta)$$
6. Compute I_E using (18).
7. $I_W = I_E + I_D$.

Table 3: Steps for Algorithm III

1-5. The Step 1 to 5 are similar to Algorithm III as given in Table 3.
6. Compute $C_0'(L_0, L_1)$ and $C_1'(L_0, L_1)$ using (4) and (5), respectively.
7. $$C_0(L_0, L_1) = \begin{cases} C_0'(L_0, L_1) & \text{if } \mathscr{X} \text{ is satisfied;} \\ C_0(L_0, L_1) & \textit{otherwise.} \end{cases}$$
$\mathscr{X} = 0.8 \times C_0'(L_0, L_1) \leq C_0(L_0, L_1) \leq 1.1 \times C_0'(L_0, L_1)$. Similarly for $C_1(L_0, L_1)$.
8. Compute I_E using (18).
9. $I_W = I_E + I_D$.

Table 4: Steps for Algorithm IV

sensor measurement and use (18) to compute I_E. The main advantage of this algorithm is that ceiling sensors provide feedback about the true illuminance in the room. Hence, it is able to resolve the issue of faulty bulb. The steps for Algorithm III are given in Table 3.

4.4 Algorithm IV

The last algorithm is similar to Algorithm III but with the additional feature of outlier rejection. Algorithm III is highly prone to error in ceiling sensor measurements especially around noon on the sunny day. The steps for Algorithm IV is given in Table 4.

5 Experiments

In this section, we shall present experimental results for the theory proposed for artificial light relationship in Section III A, daylight relationship in Section III B, and estimation algorithms in Section IV.

5.1 Artificial Light Experiments

Fig. 4(a), (b) and (c) show performance of regression analysis for the data collected at night for C_0, C_1 and hobo sensor (h) respectively. In these plots, for time instants $T = 40$ to 240, $L_1 = 0$ and L_0 is varied while for time instants $T = 260$ to 460, $L_0 = 0$ and L_1 is varied and corresponding ceiling sensors and hobo sensor measurements are recorded. As shown, the data was collected on 1, 5, 7 and 12 December and regression coefficients were estimated. We then applied the regression coefficients of each day and to the last day (12 December) data. The regression functions matches true data with minor variations. Hence, one can select any data parameters for electric light illuminance. The coefficients are tabulated in Table 5.

An important point to note in all three figures is the piece-wise linear relation of ballast levels to the illumination. The three linear links are as follows:

1. $r = 1$ indicates the low ballast level region. In this region, illumination is almost zero for zero ballast level and remain constant for ballast levels less than n_1, i.e., even though ballast level is increased from 0 to n_1, there is no increase in illumination. The low illuminance in this region can be attributed to either ambient light in the room or residual reading of sensor.

2. $r = 2$ indicates the region between n_1 and n_2 wherein illumination on work plane is directly proportional to the ballast levels, i.e., there is increase in illumination with increase in ballast level and vice versa. This is the most important region for operation of light fixtures.

3. $r = 3$ indicates the high ballast region and similar to region 1 ($r = 1$), the illumination is constant even though there is increase is ballast level beyond n_2.

Hence for most practical purposes, Region 2 ($r = 2$) is most important.

5.2 Daylight Experiments

Fig. (5) show plots for relation between sensor on the table (hobo) and window sensor (C_2). This gives us relation between daylight falling on the work plane (measured using hobo sensor) and daylight on the window. As we see, data is divided into five clusters and linear regression is performed for each cluster. Similar plots can be generated for C_0 and C_2 (see Fig. 6), and C_1 and C_2 (see Fig. 7) to understand the relation between daylight falling on the window and sensed by the ceiling sensors. Note from the plots that use of linear function is justified for the daylight models. It performs well for all the clusters. The daylight coefficients are listed in Table 6. The experimental results for daylight estimation are provided for completeness of the paper. More details can be found [8].

5.3 Estimation Experiments

We ran experiment for multiple days and show performance of algorithms for Dec 6, 2012 and Dec 9, 2012. For each day, we show estimation results, outside daylight, comparison between computed ceiling sensor and estimated ceiling sensor measurements, and changes in cluster ID. The ground truth for estimation is measured by placing a hobo sensor on the work plane. For Dec 6, all the algorithms have similar performance except Algorithm I as in Fig. 8(a). The performance of Algorithm I is mainly affected between 12:30-2:15pm. During this time, the algorithm is mainly in cluster 2 which has higher multiplier for C_0. As result, the large error measured in the C_0 for artificial light gets propagated to computations of daylight and hence overall large estimation error. One sees a small rise in the illumination on

Sensor	Parameters	$r=1$	$r=2$	$r=3$
C_0	$\begin{pmatrix} a_{00} & b_{00} \\ a_{01} & b_{01} \end{pmatrix}$	$\begin{pmatrix} 0 & 8 \\ 0 & 6 \end{pmatrix}$	$\begin{pmatrix} 1.146 & -27.847 \\ 0.726 & -15.847 \end{pmatrix}$	$\begin{pmatrix} 0.022 & 195 \\ 0 & 127 \end{pmatrix}$
C_1	$\begin{pmatrix} a_{10} & b_{10} \\ a_{11} & b_{11} \end{pmatrix}$	$\begin{pmatrix} 0 & 4 \\ 0 & 10 \end{pmatrix}$	$\begin{pmatrix} 0.496 & -11.194 \\ 1.052 & -22.513 \end{pmatrix}$	$\begin{pmatrix} -0.031 & 93.59 \\ 0 & 184 \end{pmatrix}$
h	$\begin{pmatrix} u_{00} & v_{01} \\ u_{01} & v_{01} \end{pmatrix}$	$\begin{pmatrix} 0.033 & 13.22 \\ 0.033 & 34.49 \end{pmatrix}$	$\begin{pmatrix} 1.745 & -40.568 \\ 3.231 & -66.604 \end{pmatrix}$	$\begin{pmatrix} -0.031 & 303.71 \\ -0.060 & 580.35 \end{pmatrix}$

Table 5: Relationship Coefficients for various sensors with respect to ballast levels

the work plane around 2pm even though outside daylight is reducing. This is due to change in cluster index. The blinds are fully raised in this cluster which causes some more light to enter the room. Notice in this case that this light was also sensed by ceiling sensors in Fig. 8(b).

Similar behavior is observed for Algorithm I for the experiment on Dec 9 as seen in Fig. 9. As seen from outside lux values, Dec 9 was a relatively sunnier day. Therefore around the lunch time, there was large amount of daylight in the corridor of the set up. This extra daylight was read by the ceiling sensor (C_1) which is mounted near the door. Hence, this large C_1 reading, affected the artificial light estimation (also seen in 9(b)). Hence, we see a large spike in estimation with algorithm III. However, this gets fixed in Algorithm IV as we have included a naive algorithm for outlier rejection which accounts for these large deviations. Note that Algorithm II, which does not depend on ceiling sensor measurement, has performed well in all the experiments. Algorithm II is in some sense an open loop controller and is completely dependent on the window sensor. Hence it will not be able to adapt to the daylight changes in the room.

6 Conclusion and Future Work

In this paper we present a daylight harvesting system that employs two ceiling mounted sensors inside the room, one window mounted sensor outside the room, and adjustable light fixtures and blinds. The current system has two independent controllers running, open loop controller that controls the position of blinds dependent on the solar movement, and a closed-loop controller that controls the artificial light to maintain required illumination on the work plane. We present many new algorithms to fuse information from different sensor to estimation illumination on the work plane. The proposed algorithms exploits the theory of radiosity to reduce the dimension of function approximation which leads to reduced computational demands and more accurate estimations. The proposed algorithms eliminate the need of the sensor on the work plane and therefore the sensor measurements are not affected by users. Current research can be extended in many interesting directions. First, most of the proposed algorithms have an in-built causality, i.e., estimate daylight prior to artificial light and vice versa. This leads to propagation of error. Therefore, new algorithms should be considered to eliminate it. Second, the data for daylight relationship is collected in a constrained environment (door was closed). This leads to large estimation error around noon. Therefore, data collection should be performed in a more general environment to account for various scenarios of daylight entering the room.

Acknowledgment

The author would like to thank Dagnachew Birru and Maulin Patel for their guidance in conducting this research.

References

[1] S. Selkowitz and E. Lee, "Integrating automated shading and smart glazings with daylight controls," *Lawrence Berkeley National Laboratory*, 2004.

[2] F. Rubinstein, G. Ward, and R. Verderber, "Improving the performance of photo-electrically controlled lighting systems," *Journal of the Illuminating Engineering Society of North America (IESNA)*, vol. 18, pp. 70–94, 1989.

[3] D. L. DiBartolomeo, E. S. Lee, F. M. Rubinstein, and S. E. Selkowitz, "Developing a dynamic envelope/lighting control system with field measurements," *Journal of the Illuminating Engineering Society*, vol. 26, pp. 146–164, May 1996.

[4] J. Lu, D. Birry, and K. Whitehouse, "Using simple light sensors to achieve smart daylight harvesting," *Proceeding of the 2nd ACM Worshop on Embedded Sensing Systems for Energy Efficiency in Buildings*, pp. 73–78, 2010.

[5] S. Mukherjee, D. Birru, D. Cavalcanti, S. Das, M. Patel, E. Shen, and Y.-J. Wen, "Closed loop integrated lighting and daylighting control for low energy buildings," *In Proceedings of the 2010 ACEEE Summer Study on Energy Efficiency in Buildings, Pacific Grove, CA*, 2010.

[6] E. Shen, M. Patel, and J. Hu, "Comparison of energy and visual comfort performance of independent and integrated lighting and daylight controls strategies," *ACEEE Summer Study on Energy Efficiency in Industry*, 2013.

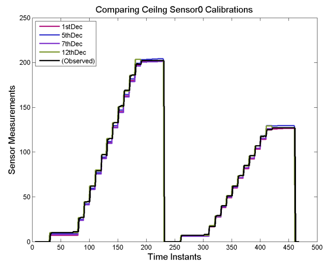

(a)

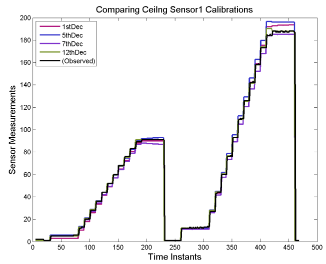

(b)

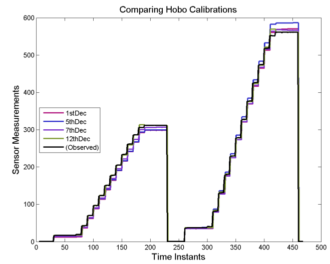

(c)

Figure 4: (a)(L_0, L_1) Vs C_0 (b)(L_0, L_1) Vs C_0 (c)(L_0, L_1) Vs h. $n_1 = 30$ and $n_2 = 210$ are used for training.

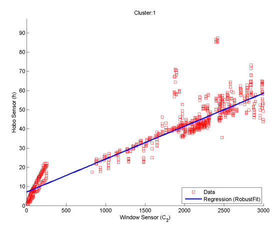

(a)

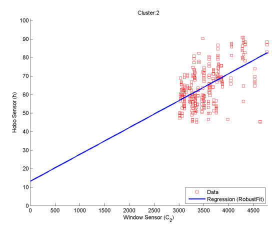

(b)

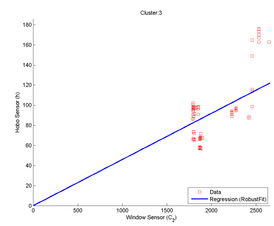

(c)

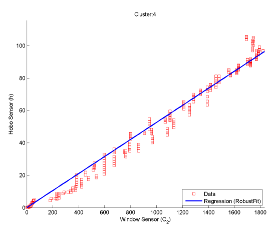

(d)

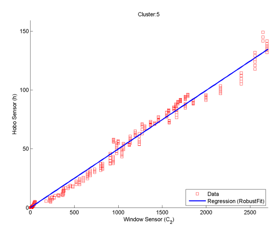

(e)

Figure 5: Hobo vs C_2 Plots (a) Cluster 1 (b) Cluster 2 (c) Cluster 3 (d) Cluster 4 (e) Cluster 5

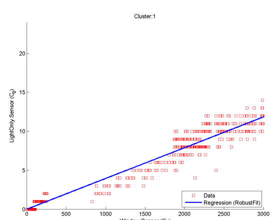

(a)

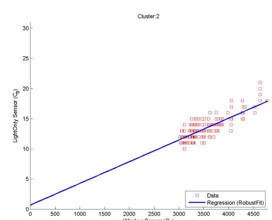

(b)

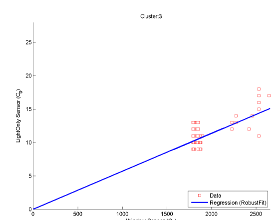

(c)

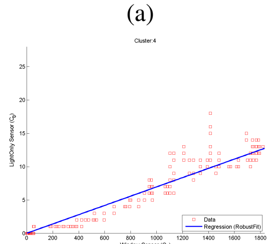

(d)

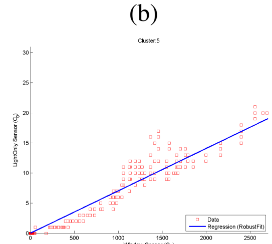

(e)

Figure 6: C_0 (Light Only Sensor) vs C_2 Plots (a) Cluster 1 (b) Cluster 2 (c) Cluster 3 (d) Cluster 4 (e) Cluster 5

Cluster Index (c)	Height (b_h) (min, max)	Angle (b_θ) (min, max)	Sunlight (C_2) (min, max)	h Vs C_2 (β_h, α_h)	C_0 Vs C_2 (β_0, α_0)	C_1 Vs C_2 (β_1, α_1)	h Vs (C_0, C_1) (β_m, α_m)
1	$(0, 0.3)$	$(-90, 90)$	$(0, 3000)$	$(7.16, 0.0171)$	$(0, 0.0039)$	$(0.930, 0.008)$	$(0, 5.0375)$
2	$(0, 0.3)$	$(-90, 90)$	$(3000, 15000)$	$(13.16, 0.0145)$	$(0.68, 0.0036)$	$(2.67, 0.0063)$	$(0, 5.0387)$
3	$(0.3, 0.8)$	$(-90, 90)$	$(0, 15000)$	$(0, 0.0459)$	$(0, 0.0056)$	$(1.64, 0.0076)$	$(0.22, 8.2798)$
4	$(0.8, 1.0)$	$(-90, 55)$	$(0, 15000)$	$(0, 0.0526)$	$(0, 0.0069)$	$(0, 0.0098)$	$(4.89, 0.7377)$
5	$(0.8, 1.0)$	$(55, 90)$	$(0, 15000)$	$(0, 0.0498)$	$(0, 0.0070)$	$(0, 0.0097)$	$(4.87, 0)$

Table 6: Table list the clustering and relationship coefficients for daylight estimation

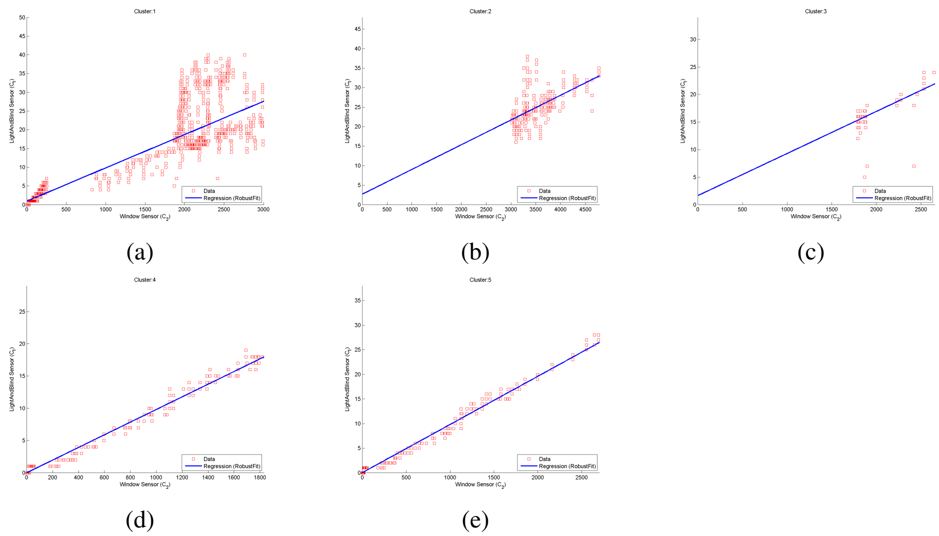

(a) (b) (c) (d) (e)

Figure 7: C_1 (LightAndBlindSensor) Vs Window (C_2) relationship (a) Cluster 1 (b) Cluster 2 (c) Cluster 3 (d) Cluster 4 (e) Cluster 5

[7] K.-W. Park and A. K. Athienitis, “Workplane illuminance prediction method for daylighting control systems,” *Solar Energy*, vol. 75, no. 4, pp. 277–284, October 2003.

[8] S. Zhang and D. Birru, “Workplane illuminance estimation for robust daylight harvesting lighting control,” October 2011.

[9] ——, “An open-loop venetian blind control to avoid glare and enhance daylight utilization,” *Solar Energy*, vol. 86, pp. 860–866, March 2012.

[10] T. Hastie, R. Tibshirani, and J. Friedman, *The Elements of Statistical Learning*. Springer, 1998.

[11] W. Hardle, M. Muller, S. Sperlich, and A. Werwatz, *Nonparametric and Semiparametric Models*. Springer Series in Statistics, 2004.

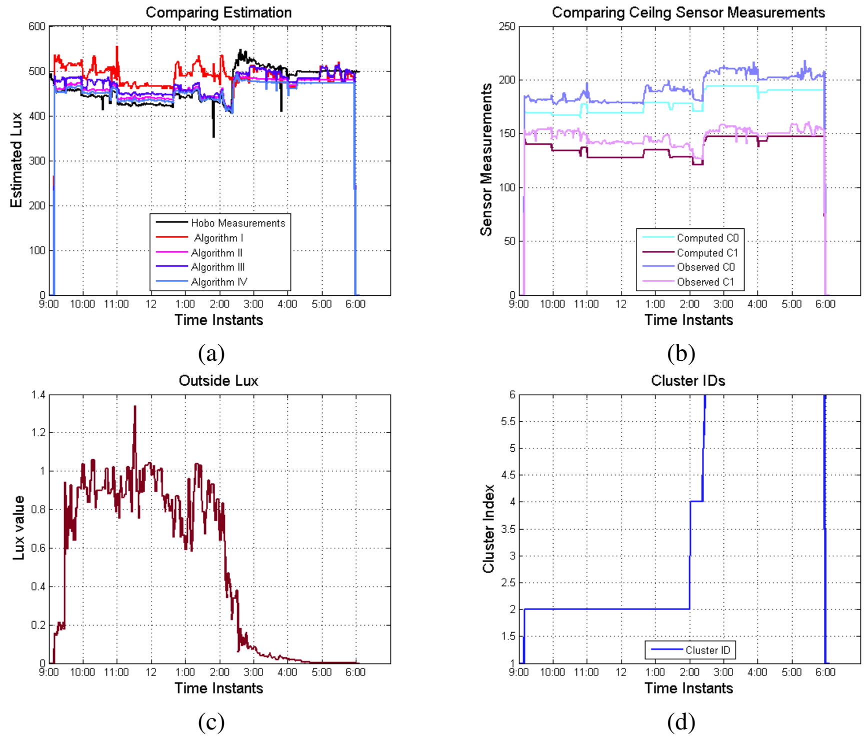

Figure 8: Simulations for 6th December 2011 (a) Estimation Results (b) Sensor Measurements (c) Window Sensor Measurements (d) Cluster ID

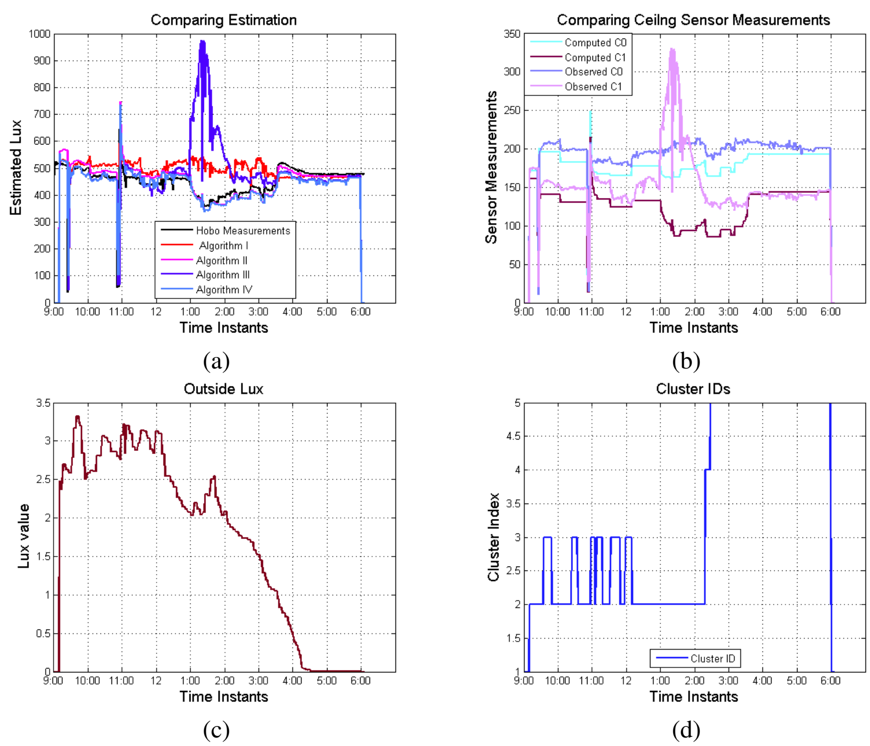

Figure 9: Simulations for 9th December 2011 (a) Estimation Results (b) Sensor Measurements (c) Window Sensor Measurements (d) Cluster ID